The Specific Interaction of Mg and Alkaline Earth Metal Ions with Well-Defined Surfaces of α-$HCrO_2$ and Cr_2O_3

Shigeharu KITTAKA,* Shigeru YAMANAKA, Naoto YANAGAWA, and Takahiro OKABE
Department of Chemistry, Faculty of Science, Okayama University of Science, 1-1 Ridaicho, Okayama 700
(Received November 4, 1989)

The selectivity sequences of Mg and alkaline earth ions to the surface of α-$HCrO_2$ and Cr_2O_3 were investigated by measuring the electrophoretic mobility and the surface charge density. The latter was determined by means of potentiometric titration. The selectivity sequence of Mg and alkaline earth ions to the α-$HCrO_2$ surface was determined as Mg>Ca>Sr~Ba. This sequence was explained by the close configurational fitting of adsorbed metal ions to the solid surface. The reason is that the O–O distance on the (001) plane of $Mg(OH)_2$ and $Ca(OH)_2$ is similar to that of the α-$HCrO_2$. On the amorphous Cr_2O_3 and crystalline Cr_2O_3, exposing mainly the (001) plane, the affinity of varying ions was comparable. The isoelectric points (IEP) of the chromium(III) hydroxide oxides and oxides were discussed in connection with their surface crystallinity as determined by electron microscopy. A lower crystallinity gives a slightly higher IEP.

The interaction of metal ions with metal oxides and metal hydroxides has been one of the most important subjects to be worked out in colloid chemistry. Accordingly, many reviews have been published on this matter.[1–4] The adsorption data have been analyzed by various complexation models involving clusters composed of adatoms and some surface atoms. However, it seems curious that any model could explain the experimental data with fairly good success to give concerted stability constants.[5] As an example, there have been reports dealing with sequences of the adsorbability of divalent cations on various solid surfaces.[1,3,6] The results obtained on the same kind of metal oxide or hydroxide did not always agree with each other. The main reason for the discrepancies seems to stem from the origin and nature of the samples. Most results were observed on the samples whose surface structures were not well-defined: neither crystal planes exposed nor crystallinity were taken account of.

As regards the surface-charge generation of metal oxide, Parks[9] has reviewed the data reported thus far and has found a simple semi-empirical relation which is a function of the charge of the metal ion, the interatomic distances, and the crystal-field stabilization energy of transition-metal ions. However, he has not considered the effects of the particle sizes on the electrification. No such works have been reported, to the present authors' knowledge. In order to solve the problems raised above, samples with well-defined surface structures and with varying particle sizes are needed.

The chromium(III) hydroxide oxide (α-$HCrO_2$) and cobalt(III) hydroxide oxide ($HCoO_2$) are hexagonal platelet particles, and both expose a well-defined (001) plane as the principal surface.[7,8] Especially, the surface of the former material was identified as atomically homogeneous, thus giving step-by-step adsorption isotherms of Kr. Particles of varying sizes can be obtained hydrothermally from $Cr(NO_3)_3$ by changing the preparation temperature and the concentration. Then, the affinity of Mg and alkaline earth ions to the surface and the variation in the isoelectric points of these samples were studied. For comparison, the surface charges of hydrous chromium oxide and anhydrous chromium oxides were also studied.

Experimental

Materials. Table 1 describes the starting materials, the conditions needed to form samples, and their surface areas, which have been determined by applying the BET equation to the amount of N_2 adsorption measured at the temperature of liquid N_2. The α-$HCrO_2$ (A1—A3) were formed by the hydrothermal hydrolysis of the $Cr(NO_3)_3$ solutions. A4 was

Table 1. Preparation and Surface Areas of α-$HCrO_2$, Cr_2O_3, and $HCoO_2$

Sample	Symbol	Preparation	Surface area/$m^2\ g^{-1}$
α-$HCrO_2$	A1	Hydrothermal hydrolysis of 0.03 mol dm^{-3} $Cr(NO_3)_3$, 120 °C, 10 days	—
α-$HCrO_2$	A2	Hydrothermal hydrolysis of 0.02 mol dm^{-3} $Cr(NO_3)_3$, 130 °C, 12 days	—
α-$HCrO_2$	A3	Hydrothermal hydrolysis of 0.3 mol dm^{-3} $Cr(NO_3)_3$, 245 °C, 1 h	39.3
α-$HCrO_2$	A4	Hydrothermal treatment of C-H, 400 °C, 1500 atm, 1 day	4.14
$Cr_2O_3 \cdot nH_2O$	C-H	Precipitation of 1 mol dm^{-3}, $Cr(NO_3)_3$ with aq NH_3	203
Cr_2O_3	C-A3	Decomposition of A3 in air, 400 °C, 4 h	31.4
Cr_2O_3	C-N	Reduction of CrO_2 with H_2, 310 °C, 2 h	—
$HCoO_2$	D	Oxidation of β-$Co(OH)_2$ in an ambient atmosphere	10.7

prepared by hydrothermally treating $Cr_2O_3nH_2O$ (C-H), which had previously been precipitated from a $Cr(NO_3)_3$ solution with ammonia water. Cr_2O_3 (C-A3) was obtained by topotactically decomposing A3 at 400 °C in air.[7] Cr_2O_3 (C-N) is a needlelike particle formed by the hydrogen reduction of CrO_2, supplied by RCA. All the materials thus prepared were purified by electrodialysis. The $HCoO_2$ was prepared by oxidizing β-$Co(OH)_2$ in an ambient atmosphere. Even after long oxidation, a small amount of Co^{2+} remained in the solid; it was then removed by treating it with 0.1 mol dm^{-3} HNO_3.

The fine structure of the samples was examined by the use of a high resolution electron microscope, JEOL JEM-2000EX. Figures 1a—1f, respectively, show the electron micrographs of A1—A4, amorphous C-H, and C-N. The particle size distributions for A1—A4 were determined by measuring the maximum diagonal distances of about four hundred particles (Fig. 2). The crystallinities of the smaller α-$HCrO_2$ particles (A1 and A2) are worse than those of the others (A3 and A4). Among chromium (III) hydroxide oxides, A3 is a well-defined hexagonal 'platelet' particle; A4 is well-crystallized, but much more polydispersed than A3. Therefore, the affinity study was mainly made on the latter sample.

Electrophoretic Mobility and Surface Charge Density. The affinity of Mg and alkaline earth ions to the solid surface was examined by measuring the electrophoretic mobility. For the measurement, a 0.5 g sample powder was suspended in

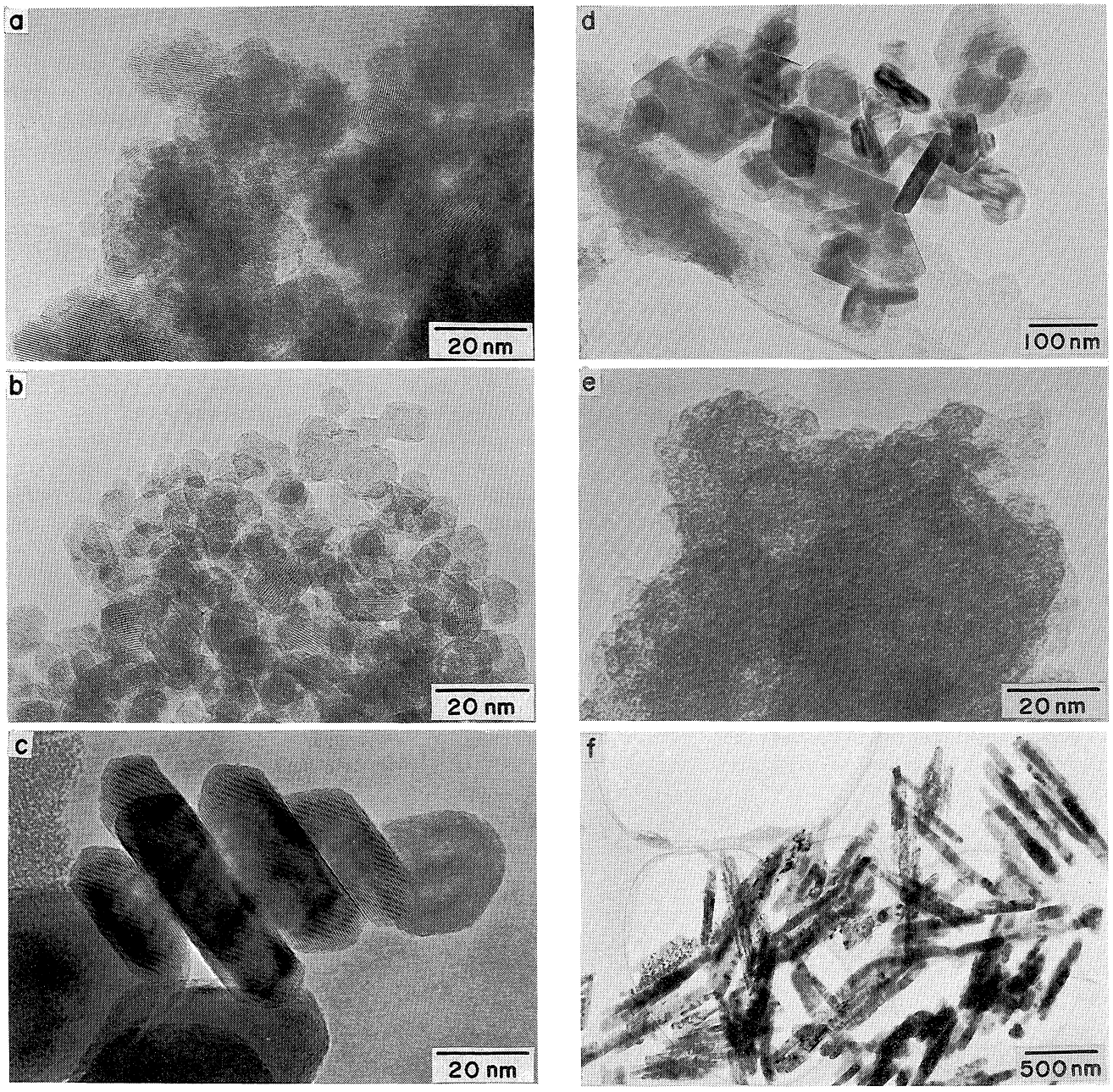

Fig. 1. Electronmicrographs of α-$HCrO_2$, $Cr_2O_3 \cdot nH_2O$ and Cr_2O_3. a, A1; b, A2; c, A3; d, A4; e, C-H; f, C-N.

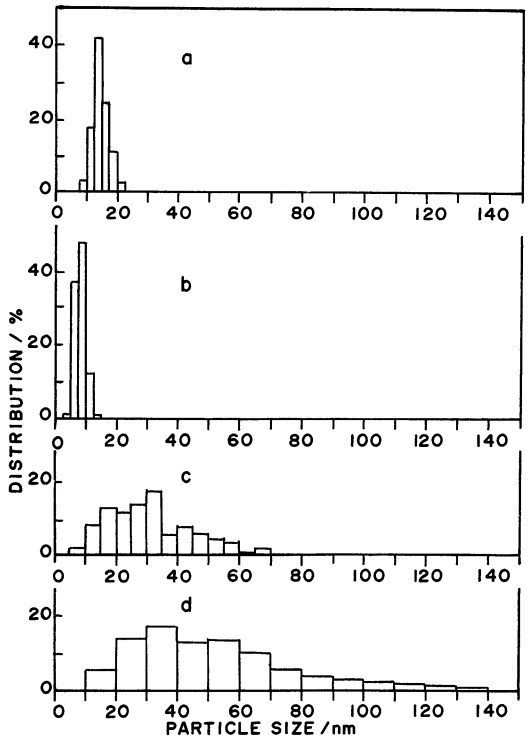

Fig. 2. Particle size distributions of α-$HCrO_2$ (A1—A4). Particle sizes are the length of their longest diagonals. a, A1; b, A2; c, A3; d, A4.

500 ml of distilled water and a portion of the suspension was mixed with an equal volume of solutions containing the desired electrolyte. The electrolyte concentration of the test solution was adjusted below 10^{-3} mol dm^{-3} so that the metal ions were not hydrolytically precipitated in the experimental range of pH 3—11. The pH of the solution was adjusted with 0.1 mol dm^{-3} HNO_3 or 0.1 mol dm^{-3} KOH. The electric field applied to the suspension in a rectangular quartz cell (1×25 mm^2) was below 10 V cm^{-1}. Forty particles were traced in their movements in the dark field. After the mobility measurements the sample suspension was transferred from the cell to the neighboring chamber to determine the pH value.

The surface charge density σ_0 was determined by conventional comparative potentiometric titration at 25 °C. A suspension of 100 cm^3, including a solid material with a surface area of 10 m^2, was titrated from about pH 4.0 by dropping in a 0.1 mol dm^{-3} KOH standard solution. The surface reaction was equilibrated within 30 min. Separately, blank titration was performed on a solution having no solid sample. σ_0 was calculated from the difference between the amounts of titrant for the test suspension (V_t) and the blank solution (V_b) at a given pH:

$$\sigma_0 = C_{OH}(V_t - V_b)F/S, \quad (1)$$

where C_{OH} is the concentration of the titrant (0.1 mol dm^{-3} KOH solution), and F, the Faraday constant. S is the surface area of the solid involved in the reaction.

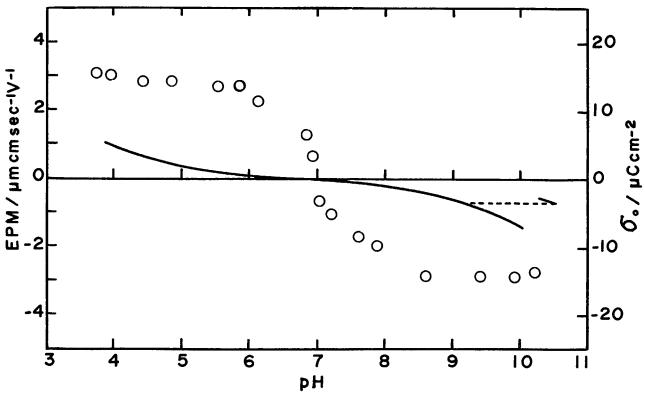

Fig. 3. Electrophoretic mobility (EPM, open circle) and surface charge density (σ_0, solid line) of α-$HCrO_2$ in 10^{-3} mol dm^{-3} KNO_3 as a function of pH.

Table 2. Isoelectric Point of α-$HCrO_2$, Mg and Cr_2O_3, and $HCoO_2$ and Sequences of Affinity of Mg and Alkaline Earth Metal Ions to Their Surfaces

Sample	IEP	Sequence
α-$HCrO_2$		
A1	7.3	
A2	7.55	
A3	7.0	Mg>Ca>Sr≈Ba
A4	6.85	Mg>Ca≈Sr≈Ba
Cr_2O_3		
C-H	7.35	Mg≈Ca≈Sr≈Ba
C-A3	6.8	Mg≈Ca≈Sr≈Ba
C-N	6.8	
$HCoO_2$	6.2	Mg>Ca>Sr≈Ba

Results and Discussion

Isoelectric Point of Chromium (III) Hydroxide Oxide and Chromium (III) Oxides. Figure 3 shows the electrophoretic mobility and surface-charge density of α-$HCrO_2$ (A3) in a 10^{-3} mol dm^{-3} KNO_3 solution as a function of the pH. Two curves cross the abscissa at pH 7.0. In other words, IEP and PZC (Point of Zero Charge) agree, indicating that neither K^+ nor NO_3^- is specifically adsorbed on the solid surface.[11] The minimum coagulation concentration was also observed at around pH=7.0 in this system (not presented here). Similar results were obtained in other systems. The IEP values for all the samples are presented in Table 2, together with the value for $HCoO_2$.

For all the many solid structures, the IEP values are confined in the narrow range of 6.8—7.55. The reported values for amorphous Cr_2O_3 are 7.0—8.4.[9,12] In α-$HCrO_2$ samples, the IEP values increase with the decrease in the particle size (Fig. 2). Noncrystalline $Cr_2O_3 \cdot nH_2O$ (C-H) has an IEP value similar to A1. The anhydrous crystalline Cr_2O_3 particles (C-A3 and C-N) have IEP values very close to those of the large

α-$HCrO_2$ (A4) particles.

The lattice fringes for the smaller α-$HCrO_2$ particles (A1 and A2) lack their completeness (Figs. 1a and 1b). This crystallographic incompleteness is due to the smaller crystal energies of ultrafine particles. Fringes for A3, A4, C-A3, and C-N are well-defined throughout the particles, although high magnification pictures have not been given for the latter three samples. These results might suggest that a smaller particle size or a lower crystallinity gives a higher IEP.

Parks[9] derived a semiempirical relation (2) for surface electrification on the metal oxide surface in aqueous systems:

$$\mathrm{IEP} = A - 11.5[(Z/R) + 0.0029B], \quad (2)$$

where A is a constant including the effects of the coordination number of metal ions composing the solid and surface hydration. Z is the valency of the metal ion, and R, the distance from the metal ion in the solid to the hydrogen via oxygen. B is a constant related to the crystal field-stabilization energy of the metal ions of the solid. It can be expected, from the poor crystallinity of the particles, that the solid is less dense than the perfect structure of a larger solid; in other words, the M–O bonds are elongated. The larger R value should lead to higher IEP values of the solids.

Specific Adsorption of Mg and Alkaline Earth Ions on the Crystalline Surface. Figure 4 shows the EPM of α-$HCrO_2$ (A3) as a function of the pH in $Mg(NO_3)_2$ solutions of varying concentrations. The positive EPM values are almost independent of the concentration of $Mg(NO_3)_2$ in the pH range below 6.0. At low $Mg(NO_3)_2$ concentrations the IEP value decreases and changes in its sign with the increase in the pH of the system. With the increase in the $Mg(NO_3)_2$ concentration, this trend is weakened and charge reversal does not occur above 10^{-4} mol dm^{-3}. This result is due to the specific adsorption of Mg^{2+} ions on the solid surface. In solutions of $Ca(NO_3)_2$ through $Ba(NO_3)_2$, the effect of the specific adsorption is less significant; the sequence of affinity is, then, Mg>Ca>Sr≈Ba for 10^{-3} mol dm^{-3} solutions (Fig. 5).

Figures 6a—6d show the relationships between the surface charge density for A3 and the pH of the solution. When the pH is increased above PZC, the decrease in negative surface charge density became more significant from Ba to Mg nitrate solutions. This sequence is comparable with the results for EPM.

The charge generation of the metal oxide surface in water, which is hydroxylated to form surface hydroxyls, has been expressed as follows under alkaline conditions:

$$M_sOH = M_sO^- + H^+ \quad (3)$$

and under acidic conditions:

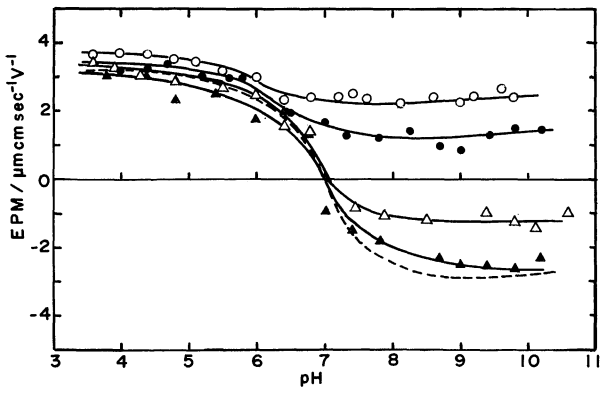

Fig. 4. Electrophoretic mobility of α-$HCrO_2$ (A3) in varying concentrations of $Mg(NO_3)_2$ as a function of pH. ○, 10^{-3} mol dm^{-3}; ●, 10^{-4} mol dm^{-3}; △, 10^{-5} mol dm^{-3}; ▲, 10^{-6} mol dm^{-3}. Broken line, 10^{-3} mol dm^{-3} KNO_3.

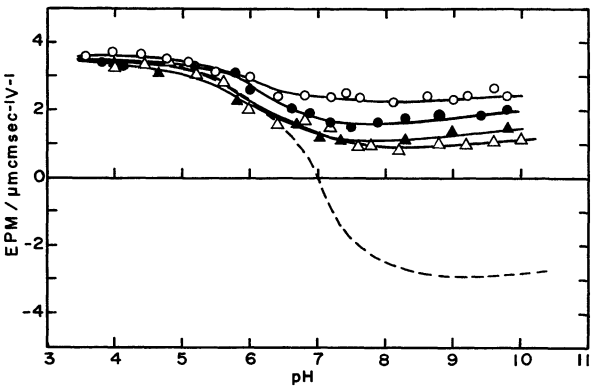

Fig. 5. Electrophoretic mobility of α-$HCrO_2$ (A3) in the Mg and alkaline earth nitrate solutions of 10^{-3} mol dm^{-3} as a function of pH. ○, $Mg(NO_3)_2$; ●, $Ca(NO_3)_2$; △, $Sr(NO_3)_2$; ▲, $Ba(NO_3)_2$. Broken line, 10^{-3} mol dm^{-3} KNO_3.

$$M_sOH + H^+ = M_sOH_2^+, \quad (4)$$

where M_s denotes the surface-metal ions of the solid used throughout this paper. These equations have been widely used to explain the amphoteric reactions of the surface, but they have not yet been confirmed experimentally. Moreover, when we consider the surface reactions from the crystallographic point of view, there are surface structures in which the two chemical reactions, (3) and (4), should not occur. One example is the present case. Oxygen ions in the (001) plane of α-$HCrO_2$ are arranged hexagonally over the chromium ions, which are also arranged hexagonally, as is shown in Fig. 7. At the electrically neutral state of the surface, half of the oxygen ions are bonded with hydrogen ions to become hydroxyls and are thus coordinated tetrahedrally by ions including underlying three chromium ions. Thus, if we consider these

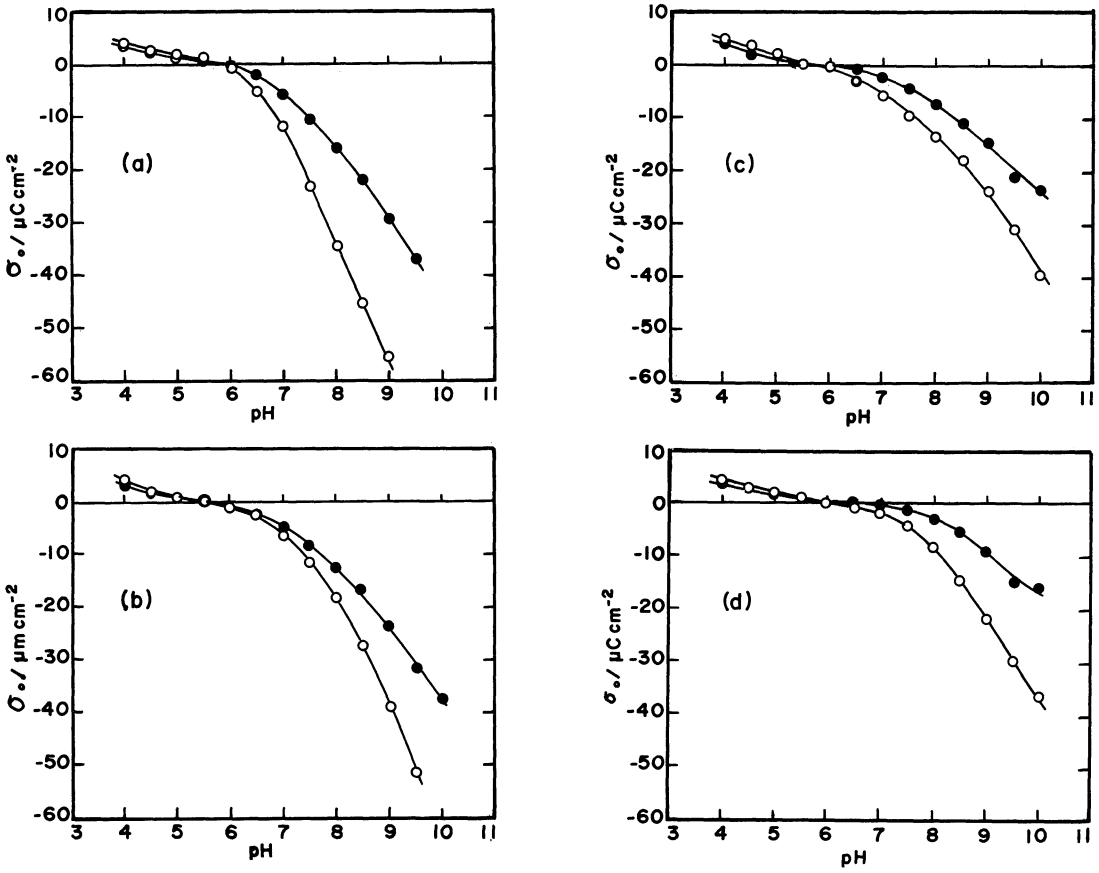

Fig. 6. Titrimetrically determined surface charge density of α-$HCrO_2$ (A3) in Mg and alkaline earth nitrate solutions (open circle, 10^{-3}, shaded circle 10^{-4} mol dm^{-3}) as a function of pH. a, $Mg(NO_3)_2$; b, $Ca(NO_3)_2$; c, $Sr(NO_3)_2$; d, $Ba(NO_3)_2$.

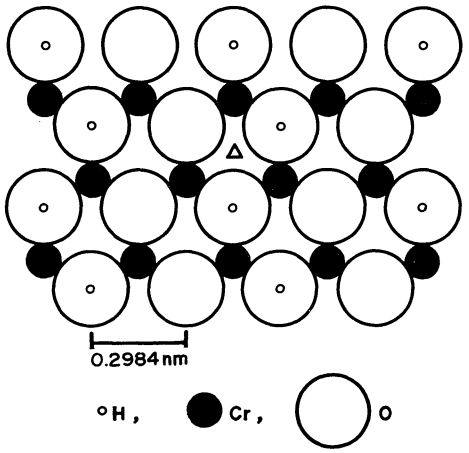

Fig. 7. Electrically neutral surface structure of α-$HCrO_2$ (001). △, a site for adsorption of metal ion.

OH groups as surface hydroxyl groups, we cannot put another H^+ on these OH groups to form the positive-surface species described in Reaction (4). The only possible points for the H^+ ions to react are bare oxygen ions on the surface. In order to bring about the charge reversal by mean of a reaction with a single H^+ ion, the following reaction may be considered to occur:

$$M_sO^{0.5-} + H^+ = M_sOH^{0.5-}. \quad (5)$$

In accordance with this, the reaction of divalent ions with the surface at a high pH can be expressed by:

$$2M_sOH^{0.5+} + M^{2+} = (M_sO)_2M^+ + 2H^+. \quad (6)$$

The equilibrium constants for Eqs. 5 and 6 are written thus:

$$K_1 = (M_sOH^{0.5+})/(M_sOH^{0.5-})(H^+), \quad (7)$$

$$K_2 = [(M_sO)_2M^+](M^+)_s^2/(M_sOH^{0.5+})^2(M^{2+}). \quad (8)$$

Here, the surface concentrations for H^+ and M^{2+}, $(H^+)_s$ and $(M^{2+})_s$, respectively, should be represented by:

$$(H^+)_s = (H^+)\exp(-e\psi^\circ/kT) \quad (9a)$$

and

$$(M^{2+})_s = (M^{2+})\exp(-2e\psi_b/kT), \quad (9b)$$

where (H^+) and (M^{2+}) are the concentrations of ions in

the bulk. ψ_0 and ψ_b are the surface potential and the potential at the Helmholtz plane respectively. Equation 8 is rewritten as:

$$K_2 = K_{ap}\exp[-2e(\psi^\circ - \psi_b)/kT], \quad (10)$$

where K_{ap} is an apparent equilibrium constant:[13]

$$K_{ap} = [(M_sO)_2M^+](H^+)^2/(M_sOH^{0.5+})^2(M^{2+}). \quad (11)$$

Furthermore, when $pQ=-\log K_{ap}$,

$$pK_2 = pQ + [2e(\psi^\circ - \psi_b)]/(2.303kT). \quad (12)$$

If the electric capacity C_1 is assumed to be constant in the Helmholtz condenser region,

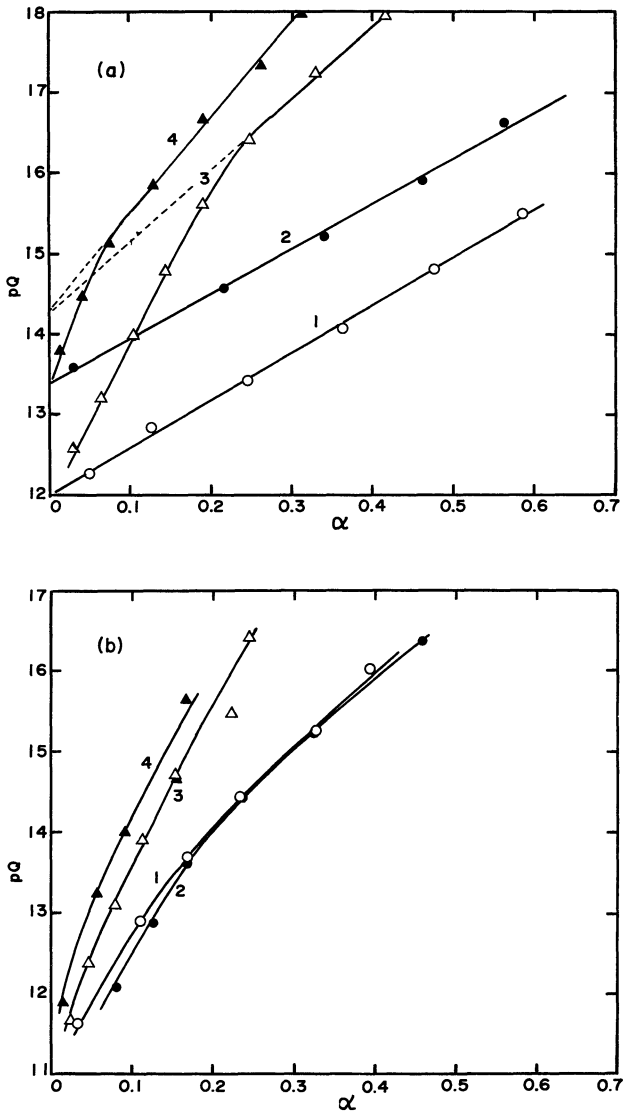

Fig. 8. The relation of $pQ(=-\log(K_{ap}))$ and degree of dissociation of surface hydroxyls, α, of α-$HCrO_2$ (A3). (1) $Mg(NO_3)_2$, (2) $Ca(NO_3)_2$, (3) $Sr(NO_3)_2$, and (4) $Ba(NO_3)_2$. Electrolyte concentrations, (a) 10^{-3} mol dm^{-3} and (b) 10^{-4} mol dm^{-3}.

$$\psi^\circ - \psi_b = \sigma_0/C_1. \quad (13)$$

As is shown in Fig. 3, the surface charge density, which has been produced simply by the reaction with H^+, is much smaller than that in the polyvalent electrolyte systems in the high pH range. Therefore, the contribution of intrinsic charge generation by Reaction (5) to σ_0 may be neglected. The degree of the dissociation of surface hydroxyls, α, is defined by σ_0/σ_f, where σ_f is the charge density described by eN_s. N_s, the density of hydroxyls on the surface, is found to be 5.93 nm^{-2} by calculating from the crystallographic data (Fig. 7). Equation 12 may be described as:

$$pK_2 = pQ - [(5.414\times10^{-4}N_s)/C_1]\alpha, \quad (14)$$

where

$$pQ = 2pH + \log\{[2(1-\alpha)^2N_s]/\alpha\} + \log(M^{2+}). \quad (15)$$

In Figs. 8a and 8b, pQ is plotted as a function of α for the higher pH range. In 10^{-3} mol dm^{-3} Mg and Ca nitrate solutions, linear relations were obtained between the two values, while in Sr and Ba nitrate solutions, the linear relation was broken at the lower α values. The pK_2 values were determined by extrapolating pQ to $\alpha=0$: 12.0, 13.4, 14.25, and 14.28 for Mg, Ca, Sr, and Ba nitrate solutions respectively. This sequence also substantiates the order of the EPM values in Fig. 5. In 10^{-4} mol dm^{-3} solutions, all the lines were curved. The departure from the linearity might be due to the decrease in the amount of divalent ions adsorbed: i.e., the contribution of the reaction (5) must be allowed for. Next we shall consider the reason why the present type of sequence was observed. Mg^{2+} and Ca^{2+} are hydrolyzed as $Mg(OH)_2$ and $Ca(OH)_2$ in high alkaline solutions respectively. These hydroxides have a brucite structure with a hexagonal symmetry. The O–O distances in the $Mg(OH)_2$ and $Ca(OH)_2$ are 0.3147 and 0.3592 nm respectively. These distances are not very large compared with that of 0.2984 nm on the (001) plane of α-$HCrO_2$. As an example, Fig. 9 illustrates the compatibility of the (001) plane of $Mg(OH)_2$ with that for α-$HCrO_2$. Mg^{2+} and Ca^{2+} are, therefore, considered to be ion-exchangeably adsorbed on the center of oxygen ions in the solid surface (Δ in Fig. 7), as if they form a hydroxide structure. Sr and Ba, on the other hand, do not form a brucite structure because of their larger ionic sizes relative to the oxygen ions. They form various types of hydroxides, such as tetragonal $Sr(OH)_2\cdot8H_2O$, orthorhombic $Sr(OH)_2H_2O$ and $Sr(OH)_2$, and monoclinic $Ba(OH)_2\cdot8H_2O$, and orthorhombic $Ba(OH)_2\cdot H_2O$ and α-$Ba(OH)_2$.[14] Then, they lack in compatibility with the α-$HCrO_2$ surface to bring about the stong specific adsorption. We propose here that the origin of the strong interactions of Mg and Ca with α-$HCrO_2$ surface is related to the

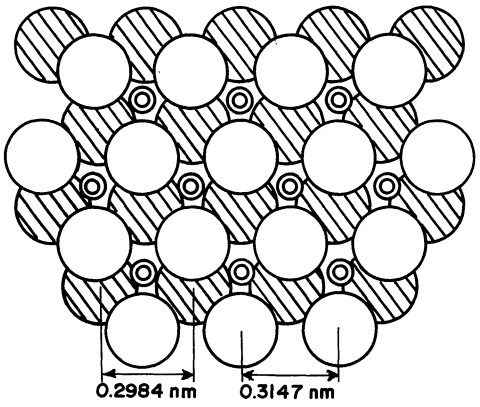

Fig. 9. Quasi-commensurated contact of (001) plane of $Mg(OH)_2$ with (001) plane of α-$HCrO_2$. Open circle, hydroxyls for $Mg(OH)_2$; small double circle, Mg ion; shaded circle, oxygen or hydroxyls for α-$HCrO_2$ surface.

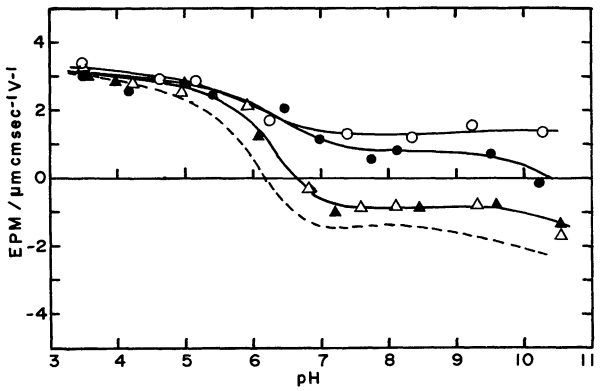

Fig. 10. Electrophoretic mobility of $HCoO_2$ (D) in Mg and alkaline earth nitrate solutions of 10^{-3} mol dm^{-3} as a function of pH. ○, $Mg(NO_3)_2$; ●, $Ca(NO_3)_2$; △, $Sr(NO_3)_2$; ▲, $Ba(NO_3)_2$. Broken line, 10^{-3} mol dm^{-3} KNO_3.

similarity between the atomic arrangements as the (001) planes of Mg and alkaline earth metal hydroxides, and of α-$HCrO_2$. This idea does not mean that Mg and alkaline earth hydroxides are formed on the surface, but that the compatibility of ions to the surface structure is responsible for the specific affinity.

This sequential adsorption was found in other systems, too. Nickel ions, which give $Ni(OH)_2$ (a=0.312 nm) of the brucite type in an alkaline solution, showed an affinity similar to that for magnesium ions. $HCoO_2$ has a skeleton (a=0.2851 nm, c=1.315 nm) somewhat smaller than that of α-$HCrO_2$. Therefore, its compatibility with Mg and Ca was worse, but a similar sequence was also found in this system (Fig. 10). Figures 11a and 11b show the results of tests of the adsorbability of divalent ions on the other chromium compounds, $Cr_2O_3 \cdot nH_2O$ (C-H) and Cr_2O_3 (C-A3) respectively. In these cases, all the

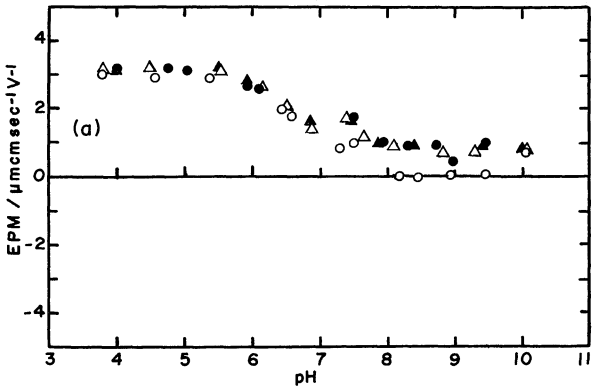

Fig. 11a. Electrophoretic mobility of $Cr_2O_3 \cdot nH_2O$ (C-H) in Mg and alkaline earch nitrate solutions of 10^{-3} mol dm^{-3} as a function of pH. ○, $Mg(NO_3)_2$; ●, $Ca(NO_3)_2$; △, $Sr(NO_3)_2$; ▲, $Ba(NO_3)_2$.

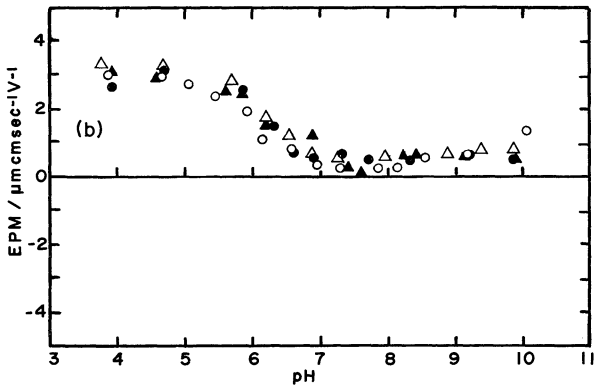

Fig. 11b. Electrophoretic mobility of Cr_2O_3 (C-A3) in Mg and alkaline earch nitrate solutions of 10^{-3} mol dm^{-3} as a function of pH. ○, $Mg(NO_3)_2$; ●, $Ca(NO_3)_2$; △, $Sr(NO_3)_2$; ▲, $Ba(NO_3)_2$.

cations have a similar affinity to these chromium oxide samples. The inability of the surface to distinguish the ions can be explained by the incompatibility of the structures between the Mg and alkaline earh ions, and the solids, i.e., the O-O distance (0.2475 nm) for the (001) plane of well crystallized Cr_2O_3 is much smaller than 0.298 nm in α-$HCrO_2$ and decisively less than 0.314 nm for $Mg(OH)_2$.

The authors wish to express their thanks to Dr. E. F. Hockings of the David Sarnoff Research Center of RCA, Princeton, N. J., for supplying the CrO_2 sample.

References

1) a) P. W. Shindler, "Adsorption of Inorganics at Solid-Liquid Interfaces," ed by M. A. Anderson and A. J. Rubin, Ann Arbor Sci. Pub., Ann Arbor (1981), p. 1. b) D. G. Kinninburgh and M. L. Jackson, *ibid.*, p. 91.

2) R. O. James and G. A. Parks, "Surface and Colloid Science," ed by E. Matijević, Plenum Press, New York and London (1982), Vol. 2, p. 119.

3) D. W. Fuerstenau, D. Manmohan, and S. Raghavan, "Adsorption from Aqueous Solutions," ed by P. H. Tewari, Plenum Press, New York and London (1981), p. 93.
4) C. P. Huang and W. Stumm, *J. Colloid Interface Sci.*, **43**, 409 (1981).
5) K. J. Farley, D. A. Dzombak, and F. M. M. Morel, *J. Colloid Interface Sci.*, **106**, 226 (1985).
6) A. Breeuwsma and J. Lyklema, *Discuss. Faraday Soc.*, **52**, 324 (1971).
7) S. Kittaka, R. Fujinaga, K. Morishige, and T. Morimoto, *J. Colloid Interface Sci.*, **102**, 453 (1984).
8) S. Kittaka, N. Uchida, I. Miyashita, and T. Wakayama, *Colloids and Surfaces*, **37**, 39 (1989).
9) G. A. Parks, *Chem. Rev.*, **65**, 177 (1965).
10) L. G. Sillen, "Stability Constant of Metal-Ion Complexes," Section 1 Inorganic Ligands, The Chemical Society, Burlington House, London (1964).
11) S. Kittaka, "Electrical Phenomena at Interfaces," ed by A. Kitahara and A. Watanabe, Marcel Dekker, New York (1984), p. 169.
12) R. Sprycha and E. Matijević, *Langmuir*, **5**, 479 (1989).
13) J. A. Davis, R. O. James, and J. O. Leckie, *J. Colloid Interface Sci.*, **63**, 480 (1978).
14) "Powder Diffraction Files, Inorganic Phases," Int. Center for Diff. Data, Parklane (1983).